Enlarged figures used in this paper

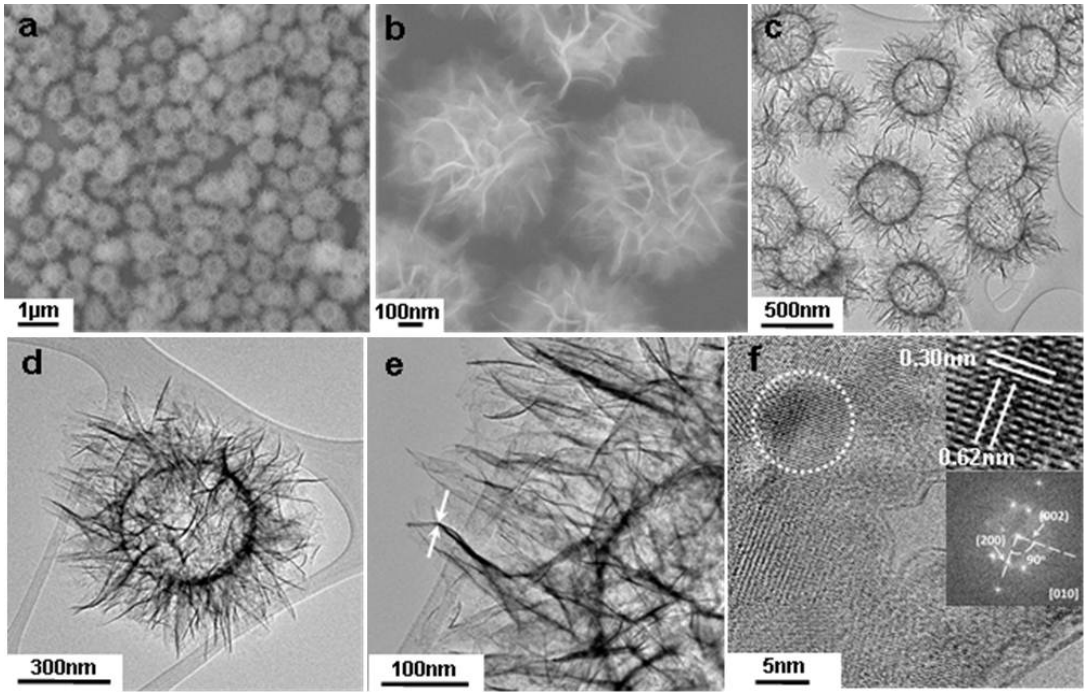

Figure 1 (a-b) FESEM and (c-f) TEM images of hierarchical hollow spheres of FeOOH composed of ultrathin nanosheets. The arrows in Figure 1e indicate the thickness of a wrinkle in nanosheets. Insets in Figure 1f: (upper) HRTEM image from the circled area; (low) the corresponding FFT image indexed to the [010] zone

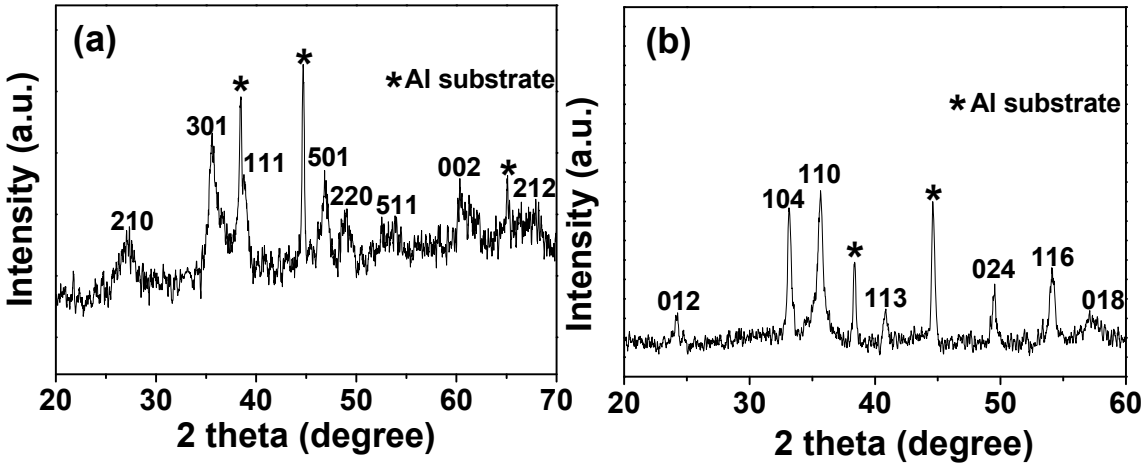

Figure 2 (a) X-ray diffraction patterns of hierarchical hollow spheres of FeOOH and (b) the hierarchical hollow spheres of Fe_2O_3 obtained after annealing at 500 ^{o}C for 10 minutes in air

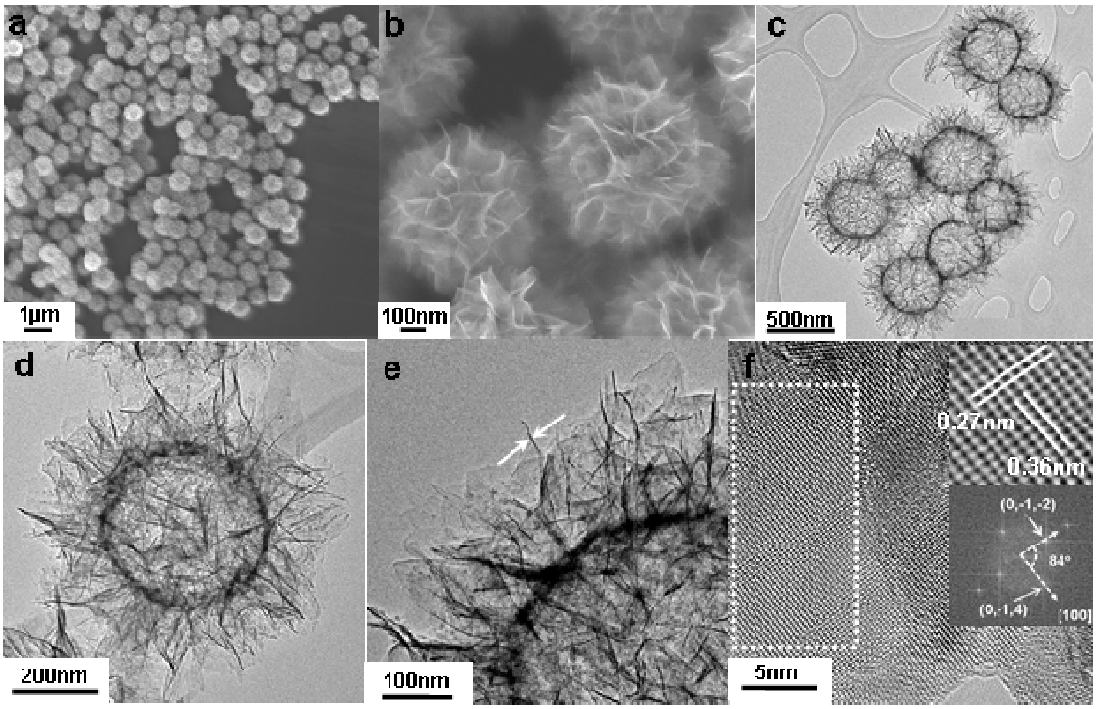

Figure 3 (a-b) FESEM images and (c-f) TEM images of hierarchical hollow spheres of α-Fe_2O_3 composed of ultrathin nanosheets. The arrows in Figure 2e indicate the thickness of a wrinkle in nanosheets. Insets in Figure 2f: (upper) HRTEM image from the rectangle area; (low) the corresponding FFT image indexed to the [100] zone

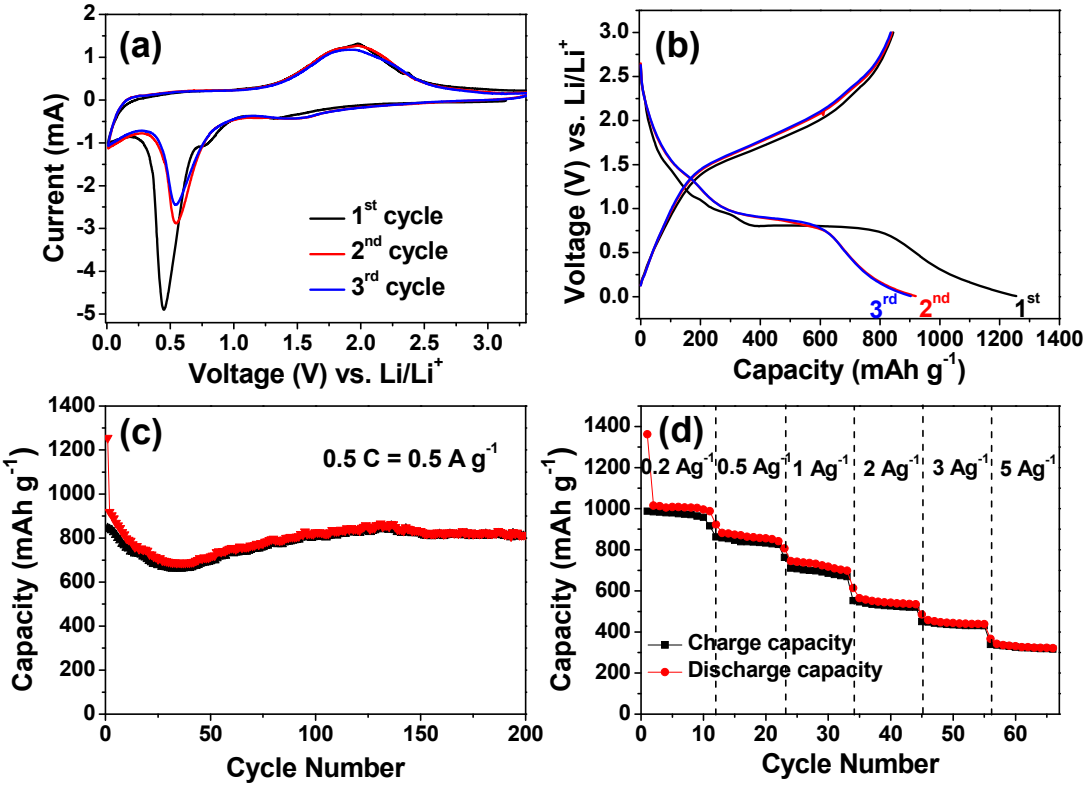

Figure 4 (a) Representative CV curves of the hierarchical hollow spheres of α-Fe_2O_3 electrode at a scan rate of 0.5 mV s^{-1} for the first, second, and third cycles, (b) Charge-discharge voltage profiles of the hierarchical hollow spheres of α-Fe_2O_3 electrode for the first, second and third cycles at a current density of 0.5 A g^{-1} (0.5 C), (c) Cycling performance of the hierarchical hollow spheres of α-Fe_2O_3 at a current density of 0.5 A g^{-1} (0.5 C), (d) Cycling performance of the hierarchical hollow spheres of α-Fe_2O_3 electrode at different current rates. Here, all cycling measurements were conducted within a voltage window of 0.01-3.0 V and 1 C is equal to 1007 mA g^{-1}

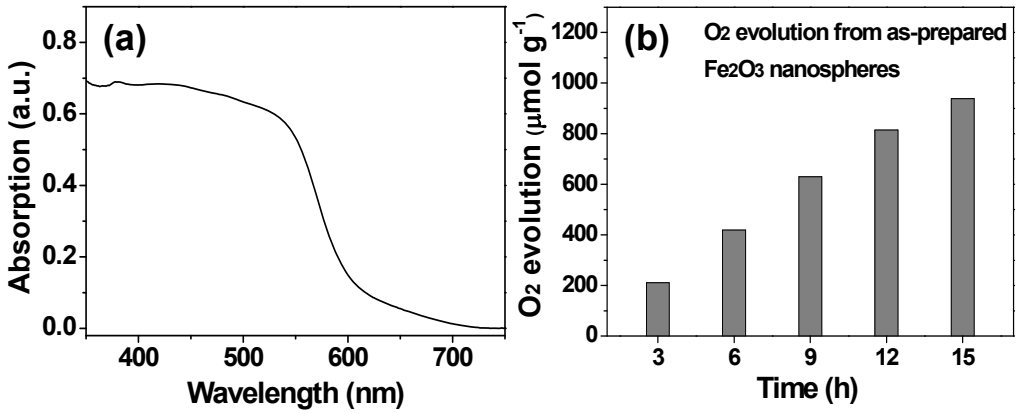

Figure 5 (a) UV-Vis absorption spectrum on hierarchical hollow sphere-based film obtained by spin coating, (b) O_2 evolution from hierarchical hollow spheres of α-Fe_2O_3 composed of ultrathin nanosheets at room temperature

Electronic Supplementary Material (ESI) for Energy & Environmental Science

Electronic Supplementary Information

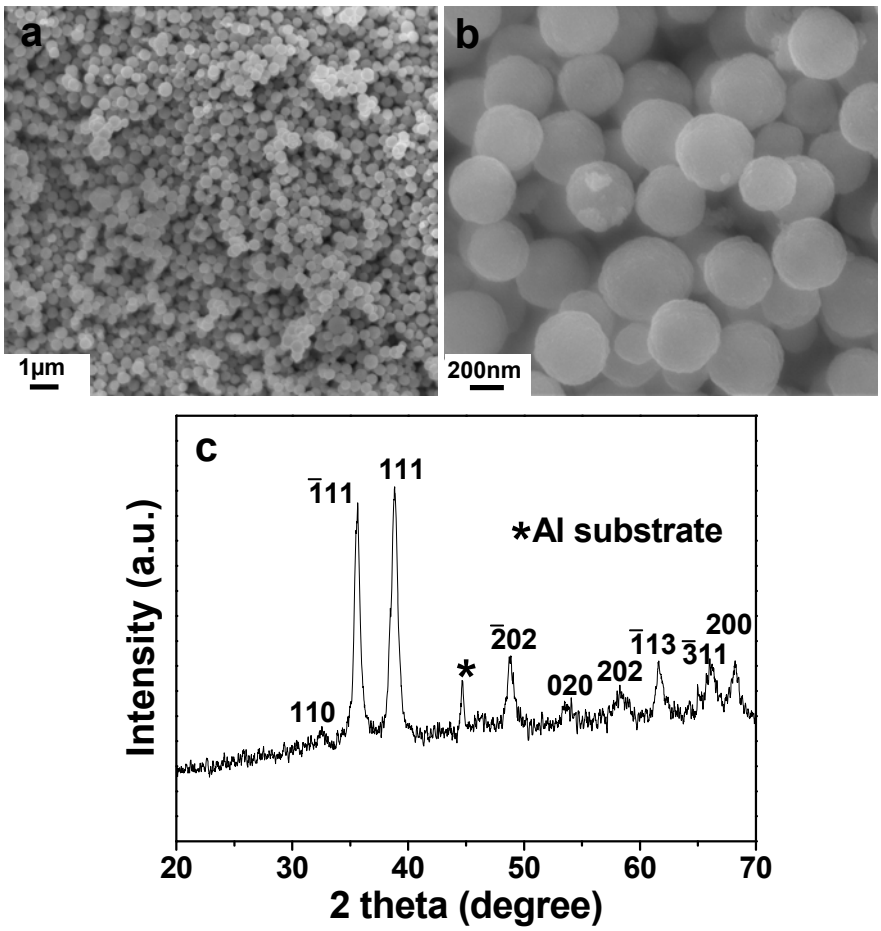

Figure S1 (a-b) FESEM images and (c) X-ray diffraction pattern of CuO spheres

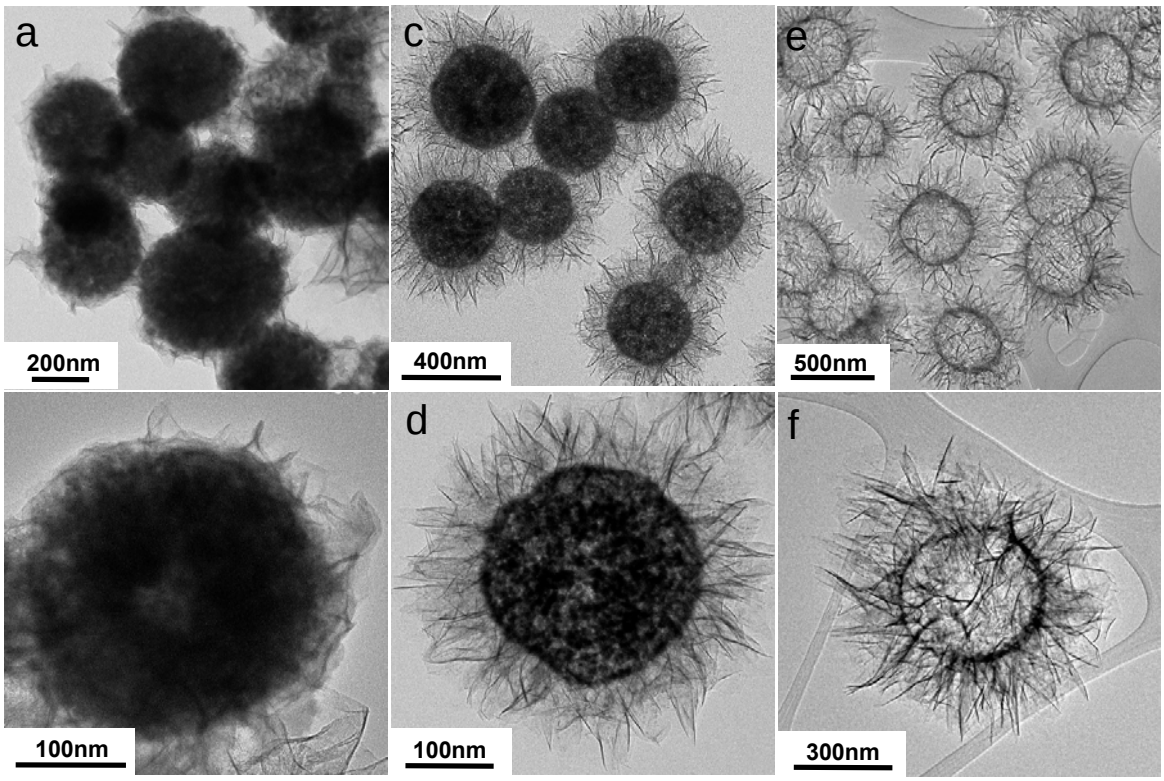

Figure S2 TEM images of the samples obtained after chemical reaction for (a-b) 15 minutes, (c-d) 30 minutes and (e-f) 60 minutes

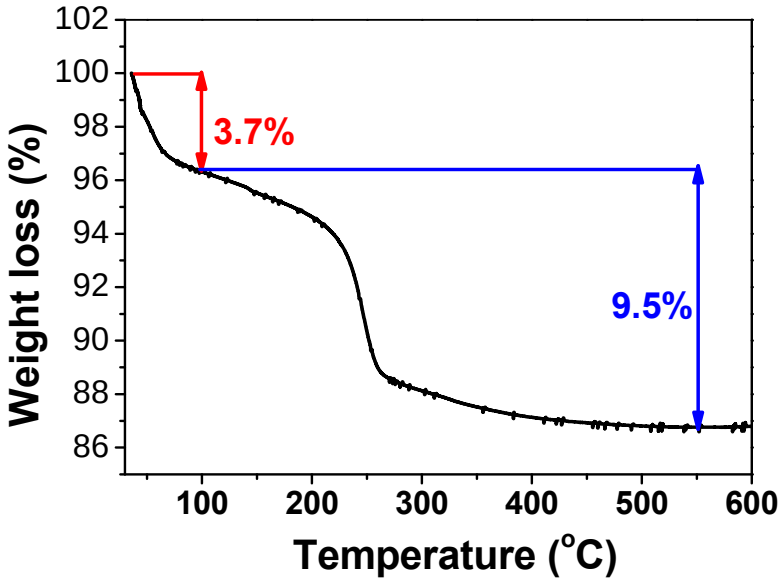

Figure S3 Thermogravimetry analyses (TGA) of the as-prepared FeOOH under an air flow with a heating rate of 10 ^{o}C min^{-1}. The weight loss of 9.5% is consistent with result calculated from the reaction: FeOOH → Fe_2O_3

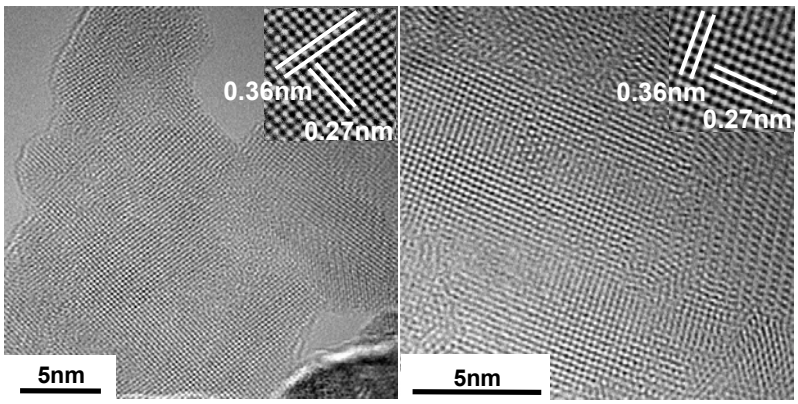

Figure S4 TEM and HRTEM images from different nanosheets of hierarchical hollow α-Fe_2O_3 spheres, showing the same lattice distances of 0.27 and 0.36 nm, corresponding to (104) and (012) planes of α-Fe_2O_3, respectively. This result is well consistent with that shown in Figure 2f

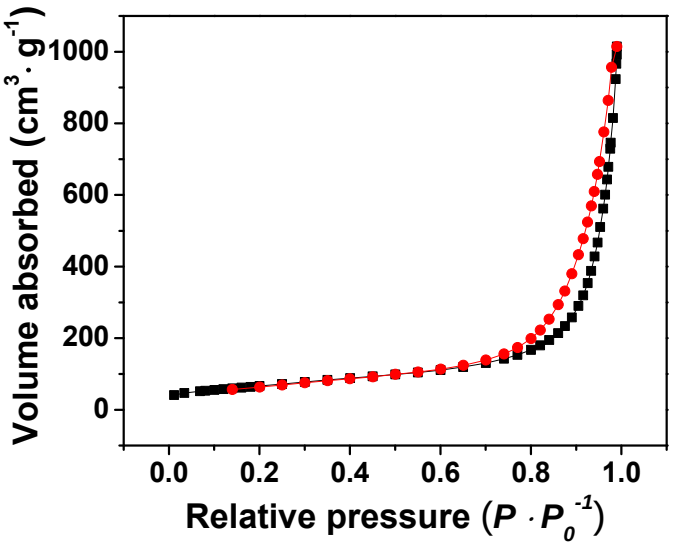

Figure S5 Nitrogen adsorption and desorption isotherms measured at 77 K for hierarchical hollow α-Fe_2O_3 spheres and the specific surface area is 139.5 m^2/g, which was calculated using the Brunauer-Emmett-Teller (BET) method.

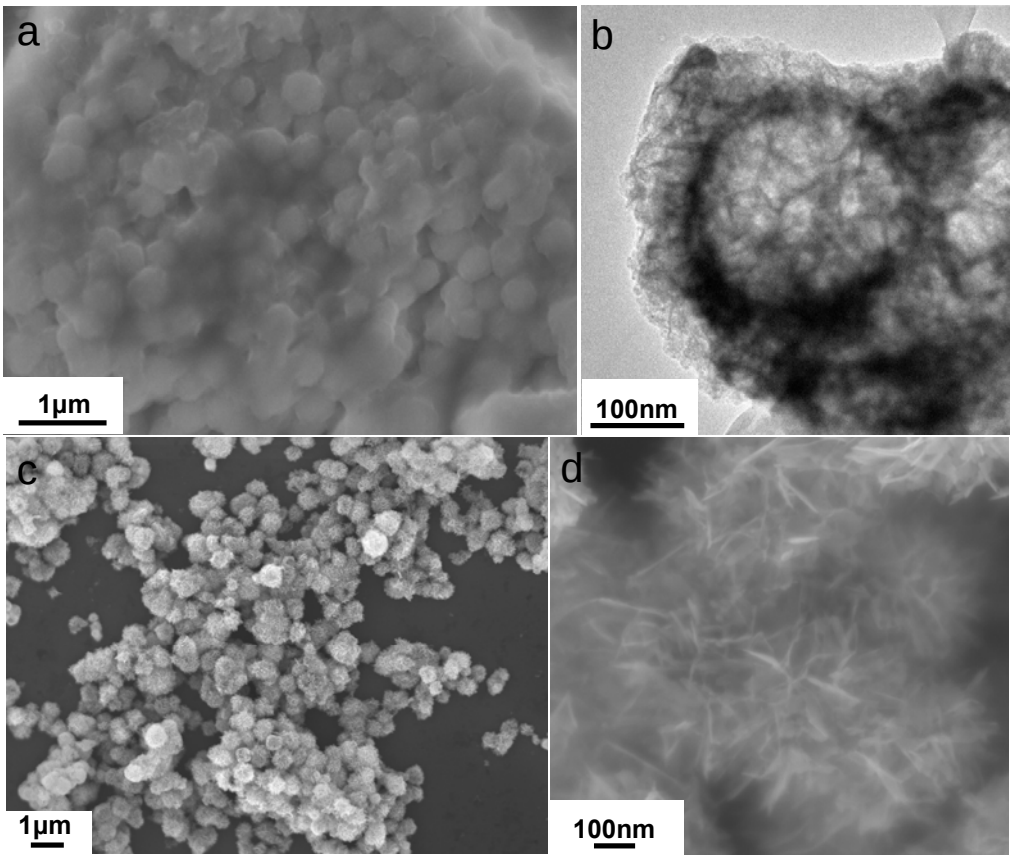

Figure S6 FESEM and TEM images of the hierarchical hollow spheres of α-Fe_2O_3 electrodes (a-b) after 200 cycles cycling test and (c-d) after photocatalytic water oxidation test

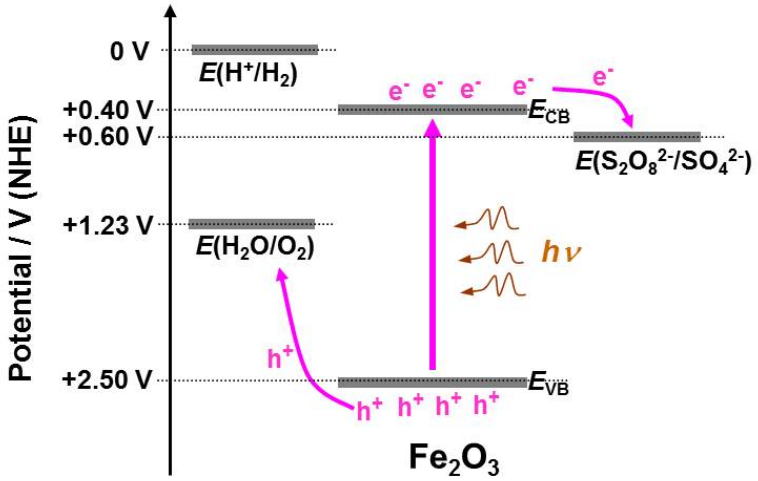

Figure S7 Schematic energy diagram for photocatalytic water oxidation with 12.6 mM $Na_2S_2O_8$ (sodium persulfate) as sacrificial electron acceptor. The conduction band edge (E_{CB}) and valence band edge (E_{VB}) of Fe_2O_3 photocatalyst at pH=7 was set at + 0.4 V and + 2.5 V *vs*. NHE, respectively.[1] The thermodynamic oxidation potential of water and reduction potential of persulfate at pH=7 was set at + 1.23 V [2] and + 0.6 V *vs*. NHE [3], respectively.

Ref:
[1] T. K. Townsend, E. M. Sabio, N. D. Browningbc and F. E. Osterloh, *Energy Environ. Sci.*, **2011**, 4, 4270.
[2] X. Chen, S. Shen, L. Guo, and S. S. Mao, *Chem. Rev.* **2010,** *110,* 6503.
[3] F. A. Frame, T. K. Townsend, R. L. Chamousis, E. M. Sabio, T. Dittrich, N. D. Browning and F. E. Osterloh, *J. Am. Chem. Soc.* **2011**, *133*, 7264.

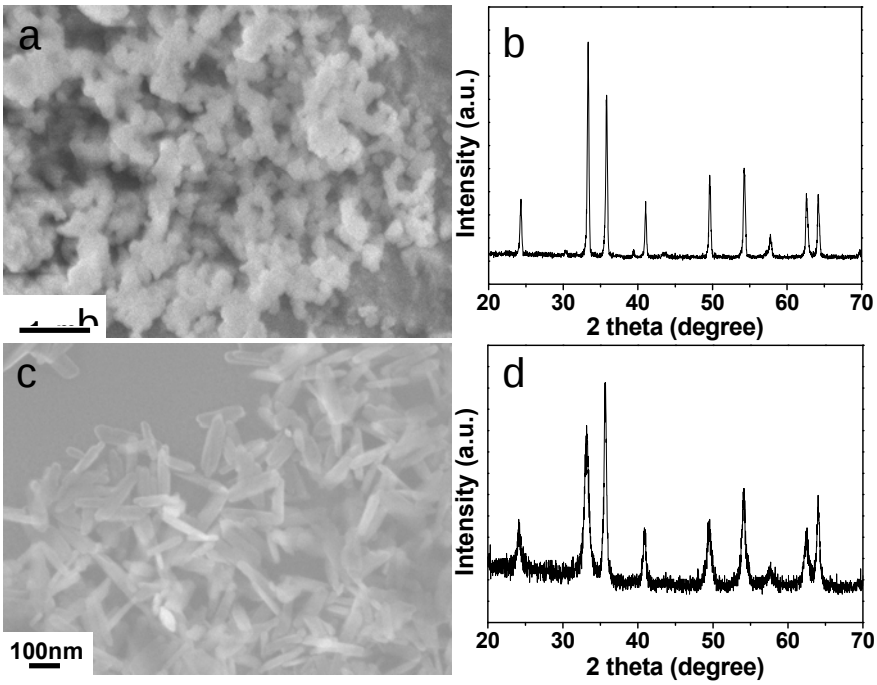

Figure S8 FESEM images and XRD patterns of (a-b) commercially-purchased Fe_2O_3 nanoparticles and (c-d) as-prepared Fe_2O_3 nanorods

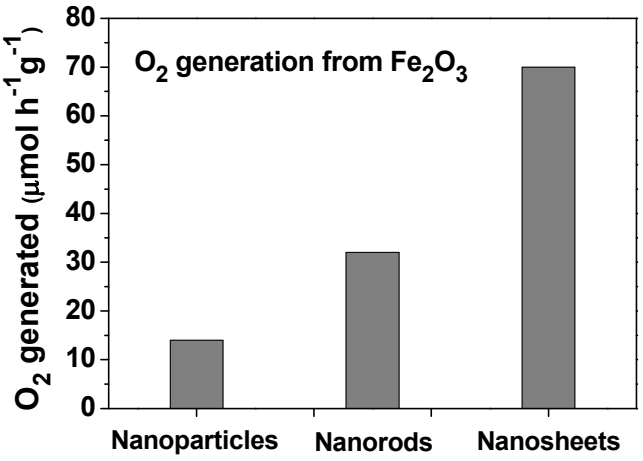

Figure S9 comparison of O_2 evolution of hierarchical hollow Fe_2O_3 spheres, as-prepared Fe_2O_3 nanorods and commercially-purchased Fe_2O_3 nanoparticles at room temperature